MONOCHROMATIZATION OPTICS FOR FCC-ee OPTIMIZED PERFORMANCE STUDY AND FIRST ATTEMPT FOR IR OPTICS DESIGN FOR FCC-ee LCC LATTICE

A. Korsun*, A. Faus-Golfe, Université Paris-Saclay, CNRS/IN2P3, IJCLab, Orsay, France

Abstract

Monochromatization is one of the most intriguing proposed operation modes of the FCC-ee, enabling a significant reduction of the centre-of-mass (CM) energy spread to a level comparable to the Higgs boson's natural width produced through the s-mode direct channel at 125 GeV. Previous studies demonstrated its feasibility using earlier versions of the FCC-ee Global Hybrid Correction (GHC) optics. A first draft implementation of the scheme on the Local Chromaticity Correction (LCC) lattice is explored in this paper. The performances of the new optics types are presented in terms of luminosity and energy spread, supported by the simulation results. This provides an early outlook on the potential operational flexibility of future FCC-ee configurations operating in monochromatization mode.

INTRODUCTION

While a significant body of previous work successfully demonstrated the feasibility of the monocromatization [1–10] scheme using various versions of the GHC lattice [11–16], this paper presents an updated implementation built upon the LCC lattice configuration with 4 IPs as the primary baseline [17]. Parametric optimization is conducted using a multi-objective optimization algorithm adapted from [18], integrating self-consistent beamstrahlung-induced emittance growth via the formulations for the beamstrahlung (BS) effect in the condition of monochromatization [19–24]. This paper is focused on implementing non-zero vertical dispersion in the interaction point (IP) D_y^*. Future studies will include performance analysis of horizontal dispersion in the IP D_x^* implementation and the hybrid mode.

ANALYTICAL OPTIMIZATION FRAMEWORK

To identify the optimal IP parameters for the monochromatization mode of the LCC lattice at 62.5 GeV, a self-consistent multi-objective optimization framework was developed. This framework relies on a numerical solver structured around the Non-dominated Sorting Genetic Algorithm II (NSGA-II) provided by the `pymoo` Python library, expanding upon the analytical methodologies for high-energy lepton colliders design [18].

The primary objective of this framework is to navigate a highly constrained, non-linear parameter space to minimize the CM energy spread (σ_w) and maximize the machine's instantaneous luminosity (L).

* anna.korsun@ijclab.in2p3.fr

Decision Variables and Physical Boundaries

The optimization framework explores a four-dimensional parameter space defined by the key adjustable variables of the IP configuration. These parameters include D_y^*, the number of bunches per beam (N_b), and the horizontal and vertical betatron functions at the IP (β_x^* and β_y^*). To ensure baseline design compatibility, these variables are scanned within the following predefined physical boundaries:

$$\vec{x} = \begin{bmatrix} D_y^* \\ N_b \\ \beta_x^* \\ \beta_y^* \end{bmatrix} = \begin{cases} 0.0 \leq D_y^* \leq 2.0\,\text{mm} \\ 2000 \leq N_b \leq 12\,000 \\ 0.09\,\text{m} \leq \beta_x^* \leq 10.0\,\text{m} \\ 0.7\,\text{mm} \leq \beta_y^* \leq 5.0\,\text{mm} \end{cases} \quad (1)$$

To maintain baseline compatibility with the overall LCC lattice design, certain parameters remain fixed during the optimization loops. The horizontal equilibrium emittance (ϵ_x) is kept constant at its purely synchrotron radiation (SR)-dominated baseline value. The vertical emittance (ϵ_y) is not parameterized independently; instead, it is calculated dynamically using a defined betatron coupling factor coupled with the localized BS blow-up. Similarly, the synchrotron tune (Q_s) is held fixed.

The design enforces a maximum allowable beam-beam parameter ceiling of $\xi_{x,y}^{\max} = 0.15$ for both planes to prevent premature beam disruption. The physical constraints are further regularized by defining a lower-bound luminosity threshold $L_{\text{target}} = 1 \times 10^{34}\,\text{cm}^{-2}\,\text{s}^{-1}$.

Self-Consistent BS Modeling and Equilibrium Parameters

A key feature of the optimization loop is the calculation of self-consistent equilibrium parameters at each genetic iteration. At 62.5 GeV, intense electromagnetic fields at the collision point trigger strong BS emissions, modifying the global bunch distributions. The underlying physics model calculates the final total energy spread σ_δ and the subsequent emittance values by iterating the self-consistent analytical formulations [19].

Because the vertical beam size in this setup is heavily dominated by the dispersive component ($\sigma_y^* \approx D_y^* \sigma_\delta$), any BS-induced increase in the energy spread creates a coupled feedback loop that directly impacts the vertical beam dimension and total luminosity. The framework evaluates these loops analytically for every generated parameter set, verifying that the resultant Pareto-optimal entries reflect true steady-state conditions.

In this model, the quantum excitation from BS during a single collision $\{n_\gamma \langle u^2 \rangle\}_{\text{BS}}$ increases both the nominal

equilibrium emittance ($\epsilon_{x,y,\mathrm{tot}}$) and the total relative energy spread ($\sigma_{\delta,\mathrm{tot}}$). These equilibrium parameters are expressed as:

$$\epsilon_{x,y,\mathrm{tot}} = \epsilon_{x,y,\mathrm{SR}} + \frac{n_{\mathrm{IP}}\tau_{x,y,\mathrm{SR}}}{4T_{\mathrm{rev}}}\{n_\gamma\langle u^2\rangle\}_{\mathrm{BS}}\mathscr{H}^*_{x,y} \quad (2)$$

$$\sigma^2_{\delta,\mathrm{tot}} = \sigma^2_{\delta,\mathrm{SR}} + \frac{n_{\mathrm{IP}}\tau_{E,\mathrm{SR}}}{4T_{\mathrm{rev}}}\{n_\gamma\langle u^2\rangle\}_{\mathrm{BS}} \quad (3)$$

where the subscript "SR" denotes the standard synchrotron radiation baseline values without BS, n_{IP} is the number of IPs, T_{rev} is the revolution period, and $\tau_{x,y,E}$ are the respective damping times.

The translation of this energy excitation into the transverse emittance depends on the IP dispersion invariant $\mathscr{H}^*_{x,y}$:

$$\mathscr{H}^*_{x,y} = \frac{\left(\beta^*_{x,y}D'^*_{x,y} + \alpha^*_{x,y}D^*_{x,y}\right)^2 + \left(D^*_{x,y}\right)^2}{\beta^*_{x,y}} \quad (4)$$

For a scheme with purely vertical monochromatization, $D^*_x = 0$, so $\mathscr{H}^*_x \approx 0$. Assuming a parallel beam at the IP ($\alpha^*_y = 0$ and $D'^*_y = 0$), the vertical invariant simplifies to:

$$\mathscr{H}^*_y \approx \frac{(D^*_y)^2}{\beta^*_y} \quad (5)$$

Because $\{n_\gamma\langle u^2\rangle\}_{\mathrm{BS}}$ is inversely proportional to the beam size and bunch length ($\sigma^3_{z,\mathrm{tot}}\sigma^{*2}_{x,\mathrm{tot}}$), the system is cross-coupled. Under the assumption of a planar designed orbit ($\tau_{x,y} = 2\tau_E$), the equations can be rewritten in a self-consistent form:

$$\epsilon_{x,y,\mathrm{tot}} = \epsilon_{x,y,\mathrm{SR}} + \frac{2V\mathscr{H}^*_{x,y}}{\sigma^2_{\delta,\mathrm{tot}}\sigma^{*3}_{x,\mathrm{tot}}} \quad (6)$$

$$\sigma^2_{\delta,\mathrm{tot}} = \sigma^2_{\delta,\mathrm{SR}} + \frac{V}{\sigma^2_{\delta,\mathrm{tot}}\sigma^{*3}_{x,\mathrm{tot}}} \quad (7)$$

where the total horizontal IP beam size is:

$$\sigma^*_{x,y,\mathrm{tot}} = \sqrt{\beta^*_{x,y}\epsilon_{x,y,\mathrm{tot}} + D^{*2}_{x,y}\sigma^2_{\delta,\mathrm{tot}}} \quad (8)$$

The introduction of the coefficient V decouples the dynamic beam-size and bunch-length terms, making V a constant determined solely by the optics design and beam parameters. For collisions with a crossing angle characterized by the Piwinski angle φ, this coefficient is:

$$V \approx \frac{55\pi^2}{3\sqrt{3}}\left(\sqrt{\frac{2}{\pi}}\right)^3 \frac{n_{\mathrm{IP}}\tau_{E,\mathrm{SR}}Q_s^2 r_e^5\gamma^2 N_b^3}{T_{\mathrm{rev}}\alpha_C^2 C^2\alpha} \times \frac{0.775\,62}{\varphi} \quad (9)$$

where r_e is the classical electron radius, γ is the Lorentz factor, α is the fine-structure constant, Q_s is the synchrotron tune, C is the circumference and α_C is the momentum compaction factor. For head-on collisions, the final factor $0.775\,62/\varphi$ is replaced by 0.7183.

Because of the non-zero vertical dispersion, the vertical beam size is dominated by the energy spread ($\sigma^*_{y,\mathrm{tot}} \approx D^*_y\sigma_{\delta,\mathrm{tot}}$). An increase in BS widens $\sigma_{\delta,\mathrm{tot}}$, which directly expands the vertical beam size, altering the luminosity and beam-beam parameters. The optimization script evaluates these equations iteratively to ensure that every calculated parameter set represents a true, stable equilibrium.

Optimization Results and Discussion

The analytical optimization script was executed to identify viable IP parameters for the monochromatization mode. While the primary target is a CM energy spread matching the Higgs boson width of 4.1 MeV [25–28], the optimization is heavily constrained by the trade-off between energy resolution and sustainable luminosity at 62.5 GeV.

Table 1 summarizes a selection of Pareto-optimal solutions identified through the multi-objective scan, while the broader dependence between energy spread, luminosity, and β_x with a fixed dispersion value $D_y = 0.5$ mm is visualized in Fig. 1. The results clearly demonstrate that decreasing the σ_W, achieved primarily by increasing D_y, comes at the severe cost of reduced instantaneous luminosity. While standard LCC Z-mode operation provides high luminosity, its natural energy spread of over 63 MeV (the baseline configuration, highlighted in bold at the bottom of the table) makes s-channel Higgs observation statistically prohibitive.

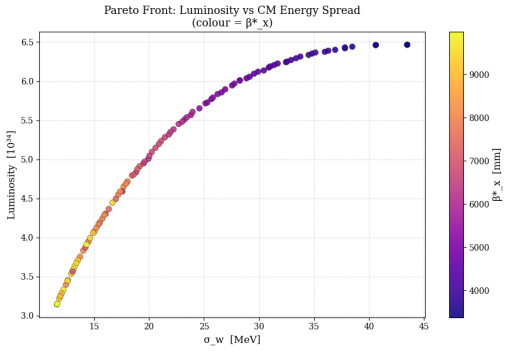

Figure 1: Dependence between σ_W and L, with the color scale indicating the value of β^*_x. Maintaining $D^*_y = 0.5$ mm.

Through our analysis, a specific configuration (marked with a † marker in Table 1) was selected as the optimal compromise. This layout achieves a significant reduction in CM energy spread (down to 11.711 MeV) while preserving a luminosity above 3×10^{34} cm^{-2} s^{-1}, providing a meaningful signal-to-background ratio. It is crucial to observe that for all viable monochromatized solutions, including our optimal selection, β_x was increased by nearly two orders of magnitude compared to the baseline (from 90 mm to nearly 10 000 mm). This drastic change is required to suppress the BS-induced emittance blow-up, and it may potentially avoid the X-Z instability zone, resulting in $\xi_x \gg \xi_y$, rotating the beam-beam tune footprint, which will be investigated in future work.

LATTICE IMPLEMENTATION

To translate the analytical optimization parameters into a realistic accelerator design, the monochromatization scheme was implemented in the interaction region (IR) of the LCC lattice. The D^*_y is generated by a set of dedicated skew quadrupole families positioned in the Final Focus System (FFS). Using the MAD-X optics code [29], the strengths of these skew quadrupoles were matched to provide the target

Table 1: Optimized IP Parameters at 62.5 GeV with 4 IPs (**Baseline**; **Optimal Monochromatization**†)

σ_W [MeV]	**L** [10^{34}cm^{-2}s^{-1}]	D_y^* [mm]	N_b	β_x^* [mm]	β_y^* [mm]	ξ_x	ξ_y	ϵ_y [pm]
63.03	**25.28**	**0**	**12 000**	**90**	**0.7**	**0.001**	**0.03**	**2.7**
9.097	1.071	1.5	11 997	9996.3	0.7	0.1051	0.0014	34.778
9.582	1.543	1.0	11 901	9974.2	0.7	0.106	0.002	18.898
10.131	2.101	0.75	11 976	9998.7	0.7	0.1056	0.0027	11.25
11.711†	**3.191**	**0.5**	**11 974**	**9996.2**	**0.7**	**0.1057**	**0.0041**	**6.519**
13.02	3.942	0.4	11 850	9990.6	0.7	0.1068	0.0051	5.386
15.014	5.016	0.35	11 023	8646.8	0.7	0.1092	0.0065	5.55
18.811	7.476	0.25	10 668	6859.3	0.7	0.103	0.0096	4.798

D_y^* = 0.5 mm for our selected optimal configuration (†). Simultaneously, the matching routine ensures that the vertical dispersion is closed outside of the IR to avoid emittance growth in the main arcs. The resulting optical functions of the modified IR, as calculated by the code MAD-X, are shown in Fig. 2.

SUMMARY AND OUTLOOK

In this paper, we presented a first-draft monochromatization scheme on the FCC-ee LCC lattice at 62.5 GeV. Combining multi-objective optimization with analytical BS modeling, we mapped the trade-offs between CM energy spread and luminosity. The required D_y^* was successfully matched in MAD-X using FFS skew quadrupoles, ensuring local dispersion closure.

Future work will expand on these findings by evaluating horizontal and hybrid monochromatization via D_x^* to compare its performance with the vertical scheme. Dedicated beam-beam simulations will also be performed to investigate the beam-beam limit, potential X-Z coherent instabilities, and the asymmetric tune footprint dynamics ($\xi_x \gg \xi_y$) inherent to these monochromatized collision parameters.

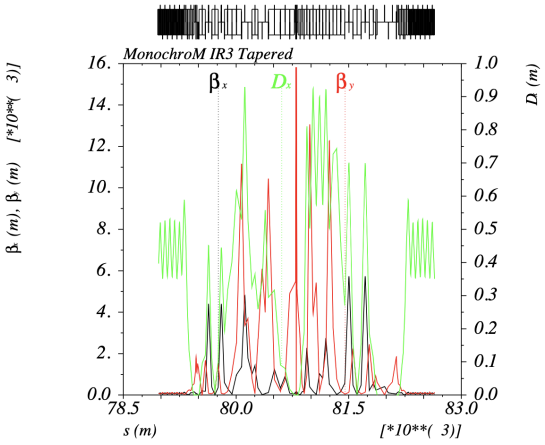

Figure 2: The matched vertical dispersion and beta functions in the LCC v105 IR modeled in MAD-X.

ACKNOWLEDGMENTS

We would like to express our gratitude to R. Soos for providing the optimization algorithm, to M.A. Jebramcik for the valuable help and guidance with the optics introduction and lattice adjustments, and to Z. Zhang for the invaluable contribution in the optics design for monochromatization, constant support, and availability. We also thank the participants of the FCC-ee meetings for their insightful discussions, feedback, and inspiration that greatly contributed to this work.

REFERENCES

[1] A. Renieri, "Possibility of achieving very high-energy resolution in electron-positron storage rings", LNF Report LNF-75/6-R, 1975.

[2] M. Bassetti *et al.*, "ADONE: present status and experiments", in *9th Intl. Conf. on High-Energy Accel.*, vol. 1, pp. 104–107, 1974.

[3] I. Y. Protopopov, A. N. Skrinsky, and A. A. Zholents, "Energy monochromatization of particle interaction in storage rings", Novosibirsk, USSR, Rep. IYF-79-06, 1979.

[4] A. A. Avdienko *et al.*, "The project of modernization of the VEPP-4 storage ring for monochromatic experiments in the energy range of psi and upsilon mesons", in *Conf. Proc. C*, vol. 830811, pp. 186–189, 1983.

[5] Y. I. Alexahin, A. N. Dubrovin, and A. A. Zholents, "Proposal on a tau charm factory with monochromatization", in *Conf. Proc. C*, vol. 900612, pp. 398–400, 1990.

[6] A. A. Zholents, "Polarized j/psi mesons at a tau charm factory with a monochromator scheme", CERN, Geneva, Switzerland, CERN Divisional Report CERN-SL-92-27-AP, 6, 1992.

[7] A. Faus-Golfe and J. L. Duff, "Versatile DBA and TBA lattices for a tau charm factory with and without beam monochromatization", *Nucl. Instrum. Methods Phys. Res. A*, vol. 372, pp. 6–18, 1996. doi:10.1016/0168-9002(95)01275-3

[8] A. A. Zholents, "Sophisticated accelerator techniques for colliding beam experiments", *Nucl. Instrum. Methods Phys. Res. A*, vol. 265, pp. 179–185, 1988.

[9] K. Wille and A. W. Chao, "Investigation of a monochromator scheme for SPEAR", SLAC, Stanford, CA, USA, SLAC Technical Report SLAC/AP-032, 1984.

[10] M. Bassetti and J. M. Jowett, "Improving the energy resolution of LEP experiments", in *Conf. Proc. C*, vol. 870316, Washington D.C., USA, p. 115, 1987.

[11] Z. Zhang, A. Faus-Golfe, *et al.*, "Monochromatisation optics for FCC-ee lattices", in *CEPC Workshop 2023*, 2023. https://indico.ihep.ac.cn/event/19316/contributions/142896/

[12] Z. Zhang, A. Faus-Golfe, *et al.*, "Monochromatization interaction region optics design for direct s-channel production at FCC-ee", Venice, Italy, pp. 738–741, Sep. 2023. doi:10.18429/JACoW-IPAC2023-MOPL079

[13] Z. Zhang, "Interaction region optics design of a monochromatization scheme for direct s-channel Higgs production at FCC-ee", Ph.D. thesis, U. Paris-Saclay, Orsay, France, 2024.

[14] Z. Zhang *et al.*, "Update in the optics design of monochromatization interaction region for direct Higgs s-channel production at FCC-ee", in *Proc. IPAC'24*, Nashville, TN, USA, pp. 2520–2523, Jul. 2024. doi:10.18429/JACoW-IPAC2024-WEPR21

[15] Z. Zhang, A. Faus-Golfe, *et al.*, "Optimized physics performance evaluation of monochromatization interaction region optics for direct s-channel higgs production at FCC-ee", in *Proc. IPAC'25*, Taipei, Taiwan, pp. 406–409, Nov. 2025. doi:10.18429/JACoW-IPAC25-MOPM040

[16] Z. Zhang, A. Faus-Golfe, A. Korsun, *et al.*, "Monochromatization interaction region optics design for direct s-channel higgs production at FCC-ee", *Nucl. Instrum. Methods Phys. Res. A*, 2025. doi:10.1016/j.nima.2025.170268

[17] P. Raimondi, S. M. Liuzzo, L. Farvacque, S. White, and M. Hofer, "Local chromatic correction optics for future circular collider e^+e^-", *Phys. Rev. Accel. Beams*, vol. 28, no. 2, p. 021002, Feb. 2025. doi:10.1103/PhysRevAccelBeams.28.021002

[18] R. Soós, "Performance limitations due to beam-beam interactions and wakefields in high energy lepton colliders", Ph.D. thesis, U. Paris-Saclay, Orsay, France, 2026. doi:10.70675/7925b569zcd8cz49f2z8e3dz6b334f2-fc30e

[19] M. A. V. García and F. Zimmermann, "Beam blow up due to beamstrahlung in circular e+e- colliders", *Eur. Phys. J. Plus*, vol. 136, p. 501, 2021. doi:10.1140/epjp/s13360-021-01485-x

[20] M. A. V. García and F. Zimmermann, "Effect of emittance constraints on monochromatization at the Future Circular e+e- Collider", in *Proc. IPAC'19*, Melbourne, Australia, 2019. doi:10.18429/JACoW-IPAC2019-MOPMP035

[21] M. A. V. García and F. Zimmermann, "Towards an optimized monochromatization for direct higgs production in future circular e+e- colliders", in *CERN-BINP Workshop for Young Scientists in e+e- Colliders*, pp. 1–12, 2017. doi:10.23727/CERN-Proceedings-2017-001.1

[22] F. Zimmermann and M. A. V. García, "Optimized monochromatization for direct Higgs production in future circular e+e- colliders", in *Proc. IPAC'17*, Copenhagen, Denmark, WEPIK015, p. 4, 2017. doi:10.18429/JACoW-IPAC2017-WEPIK015

[23] T. Sen, "Luminosity and beam-beam tune shifts with crossing angle and hourglass effects in e^+-e^- colliders", Rep. FERMILAB-FN-1175-AD, Aug. 2022. doi:10.2172/1958796

[24] M. A. V. García, D. E. Khechen, K. Oide, and F. Zimmermann, "Quantum excitation due to classical beamstrahlung in circular colliders", in *Proc. IPAC'18*, Vancouver, Canada, 2018. doi:10.18429/JACoW-IPAC2018-MOPMF068

[25] M. Mangano *et al.*, "FCC physics opportunities", *Eur. Phys. J. C*, vol. 79, no. 6, p. 474, 2019. doi:10.1140/epjc/s10052-019-6904-3

[26] A. Abada, M. Abbrescia, S. S. AbdusSalam, M. Benedikt, *et al.*, "FCC-ee: the lepton collider", *Eur. Phys. J. Spec. Top.*, vol. 228, p. 261, 2019. doi:10.1140/epjst/e2019-900045-4

[27] S. Jadach and RA. Kycia, "Lineshape of the Higgs boson in future lepton colliders", *Physics Letters B*, vol. 755, pp. 58–63, Apr. 2016. doi:10.1016/j.physletb.2016.01.065

[28] FCC-FS EPOL group meeting, https://indico.cern.ch/event/1108961

[29] MAD-X - methodical accelerator design, http://madx.web.cern.ch/madx/